Anonymous Referee #1:

We sincerely appreciate for your time and attention on our paper. The comments and suggestions you gave are very helpful for us to improve our paper. We now present point-by-point replies (in black) to all your comments (in green) in this response and the corresponding changes in the revised manuscript have been highlighted in blue.

- **Experimental Description:**

1. Define the geographic limits of the North China Plain.

Reply: The NCP region includes Beijing, Tianjin, and most of Hebei province, which is surrounded by Taihang Mountains to the west, Yanshan Mountains to the north, and Bohai Sea and Yellow Sea to the east with Korea and Japan farther east of the Yellow Sea.

We have added a China Map to show the location of the North China Plain region in the revised manuscript.

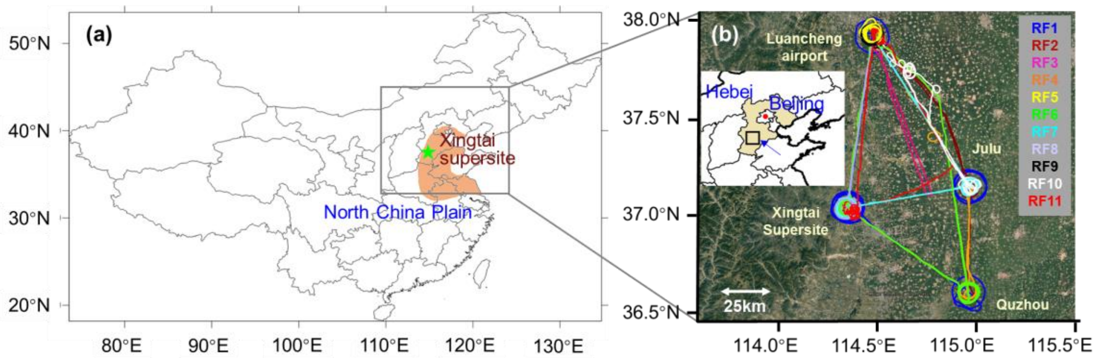

Fig.1 Map of the geographic location of North China Plain and the Xingtai supersite (a), and the flight tracks of the 11 research flights conducted over Hebei Province in May-June 2016 (b).

2. What is the relevance of the NCP to the rest of China and Northeast Asia (other than being densely populated and fast developing - these two characteristics could be used to describe most anywhere in China)?

Reply: The NCP region is the most polluted area in China and Northeast Asia. With great industrial activity and increase in automobiles during the last several decades, the consumption of fossil fuels like coal, gasoline, diesel, and natural gas has increased dramatically in this region. The combustion of fossil fuels emits large amounts of particulate and gaseous pollutants into the atmosphere, leading to substantial environmental problems. Industrial and automobile related primary emissions, as well as the formation of secondary aerosols, combined with the transport of dust from the desert region in Northwest China, result frequently in heavy aerosol loads in the NCP depending on the meteorological conditions. In this area, air quality is significantly influenced by aerosol particles and high loads of aerosol pollution severely degrade visibility, especially under high RH conditions.

Besides being one of the most populated region with fast economic development that generate huge anthropogenic emissions, the region has a unique topography which, together with weather regimes, plays an important role in regulating air pollution and in return influences the regional climate. With a mountain range to the west (Yan and Taihang mountains), any easterly and southerly winds may bring in and accumulate pollutants in both particulate and gas phases. Blocking of the polluted air mass may not only affect the boundary-layer condition by altering thermodynamic state but also induce a conditional instability to induce heavy rainfall as reported in another study of similar topographic setting (Fan et al., 2015). These features make the NCP to be a unique area to study emissions of air pollutants and their transport to surrounding areas in China and Northeast Asia.

3. ***What is the motivation behind the location of the surface supersite, the flight paths, locations for spirals, and the frequency of flights?***

Reply: There are a few reasons we choose Xingtai as a surface supersite station. First of all, it represents the typical geographical features and air pollution characteristics of the NCP regions, as shown in the responses to Comments 1& 2s. Statistics shows that Xingtai and other southern Hebei cities were among the worst-ranked cities by seasonal or annual air quality index in 2013 and 2014 (Li et al., 2015). Secondly, as a national primary weather station, basic meteorological parameters and sounding observations have been made at the Xingtai supersite routinely. Lastly, it has existing infrastructure to support the field experiment.

As the base airport for this experiment was located in Luancheng, Shijiazhuang, and considering the combination of aircraft and surface observations, most of our research flights, focus on vertical distribution of air pollutants, were conducted over Luancheng and Xingtai. Due to restrict control of airspace in this area, we choose Julu and Quzhou as different underlying surface conditions for comparison. As we usually conduct observation of aerosol optical properties under cloudless day, the flight design and its frequency were determined by weather conditions and airspace availability.

4. ***What is the relevance and motivation for the time period of the flights?***

Reply: The overall period of our flights is dictated by the duration of the entire experiment that was chosen in light both the regional climate and in cooperation with another major international experiment, the NASA KORUS-DAQ campaign, in downwind South Korea (Al-Saadi et al., 2016). The dates and time of any individual flights were determined by weather regimes and aerospace availability, and often the latter being more crucial due to difficulties in getting any. Weather-wise, NCP region is characterized by a warm temperate monsoon climate, dominated by the northern cyclones and cold fronts in the spring, resulting in strong wind, and precipitation by convection is mainly concentrated in summer (Sun et al., 2013). To avoid the strong wind and convective precipitation, the experiment was carried out in May and June, which could essentially represent the aerosol conditions from spring to summer in the NCP region.

5. ***How representative are the measurements of the NCP region during these two months?***

Reply: Two experimental aircrafts were deployed during the in-situ campaign, a Y-12 and a Cheyenne-III (C-III). The Y-12 flights mainly focused on atmospheric pollutants under cloud-free conditions. The Cheyenne-III was equipped with a suite of instruments for cloud and precipitation measurements. The following table lists weather conditions during the experiment. We carried out the flight experiments under a variety of weather (cloudy, rainy, or strong wind) and air pollution (clear, hazy, heavily polluted) conditions over the 2-month period, so the measurements are representative for the level of pollution and aerosol optical properties in the NCP region.

Table 1 An overview of flight information and the weather phenomenon by ground measurement during the experimental period.

date	flight or not		weather of LC Airport	date	flight or not		weather of LC Airport
	Y-12	C-III			Y-12	C-III	
0508	√		haze	0526			clear
0509			light rain	0527			overcast
0510			haze	0528	√√	√	clear
0511			heavy polluted	0529			clear
0512			overcast	0530			haze
0513			overcast	0531			clear
0514			rainfall	0601			haze
0515	√		clear	0602	√		heavily polluted
0516	√		clear	0603		√	overcast
0517	√		haze	0604		√	rainfall
0518			haze	0605		√√	rainfall
0519	√		heavily polluted	0606	√		haze
0520			haze	0607			heavily polluted
0521	√	√	haze and light rain	0608			haze
0522			haze	0609			heavily polluted
0523		√	rainfall	0610			thunder
0524			very strong wind	0611	√		clear
0525			overcast				

6. ***What were the general meteorological conditions during the campaign? Clear? Overcast? Stagnant? What are the prevailing winds? Do you expect long-range transport during this time period?***

Reply: The meteorological conditions during the flight campaign are shown in Table 1. Generally, we carried out the aerosol optical observations during daytime under variable air quality conditions from very clean to rather hazy conditions. The prevailing winds were northwesterly or westly that brought dry and clean airmasses from less polluted areas to the experimental region. The long-range transport of air pollutants occurred when the wind direction changed. For example, easterly or southerly winds brought pollutant plumes to the study region, which lead to the occurrence of pollution events. Similarly, under weak wind conditions, the stagnant conditions caused multi-day air pollution episode.

- **Section 4.1:**

7. ***How was clean PBL defined? Which flights/spirals/dates were identified as clean?***

Reply: We defined the clean PBL where the mean value of σ_{sca} below 100 Mm^{-1} at every 100m and low levels of gas pollutants like CO and NOx were observed. Based on this definition, the clean flights/spirals on different dates include RF1 (on May 8, spirals at JL, XT), RF4 (on May 17, spirals at JL, QZ) and RF11 (on June 11, spirals at LC, XT), about 13 vertical profiles in total.

8. ***What is the purpose of Eq 6? Did you calculate the scale height? What is it?***

Reply: The purpose of Eq.6 was considered as follows. When the σ_{sca} profiles in clean PBL cases are taken as an ensemble, and they fit nicely on a diagram, the σ_{sca} profiles are transformed into a parameterized model. The scale height is now calculated in Eq. (8) as the height when σ_{sca} is reduced to 1/e of its surface value. We have added the following description in Section 4.1 of the revised manuscript:

The mean σ_{sca} profile decreases exponentially with height, which can be expressed as:

$$\sigma_{sca,H}=\begin{cases}\sigma_{sca,0}\cdot\exp(-(H-H_{RS})/H_p), & (\text{if } H > H_{RS})\\ \sigma_{sca,0}, & (\text{if } H \leq H_{RS})\end{cases}, \quad (6)$$

where $\sigma_{sca,0}$ is σ_{sca} measured at the surface, H is the altitude above sea level, and H_p is the aerosol scale height (H_p represents the height when σ_{sca} is reduced to 1/e of its surface value); H_{RS} represent a relative stable layer near surface where the vertical variation of σ_{sca} was not significant. In the cases of a typical clean PBL, $\sigma_{sca,0}$=124 Mm^{-1}, H_p =1146 m and H_{RS} =837 m. The linear regression analysis suggests a correlation coefficient, r^2=0.96.

9. ***What is the significance of there being high correlation between RH and sigma_scat at low RH, but not at high RH? How many profiles are you basing this correlation off of?***

Reply: The establishment of the correlation between σ_{sca} and RH, mainly considering the vertical distribution of aerosol optical properties (hard to get) could be calculated by means of the measurement of RH profiles (easy available) during this field campaign. We can also estimate the source of corresponding air masses by the back-trajectory analysis.

In the clean PBL conditions, there were 11 profiles in total basing this correlation. We can infer that if the measured RH profile was in accordance with RH_dry profile in

Fig.6c (in the revised manuscript), the σ_{sca} distribution was shown in correspond in Fig.6a, and the air mass most commonly originated from Northwest China by long-range transport. There was a poor correlation (r^2=0.23) between RH and σ_{sca} in the case of higher RH condition (RH>50), but we could conclude that the surface layers are relatively stable and the pollutants were mainly from emissions in local or the surrounding areas.

10. ***In general, it is not clear what data is plotted in Figure 9.***

Reply: We make a linear regression analysis between airborne measured ambient RH and σ_{sca} (550nm) profiles in Fig. 9 (now Fig. 8 in the revised manuscript). The scatter, the horizontal and vertical error bars represent mean values and the standard deviations of RH and σ_{sca} at every 100m level. For example, under clean PBL condition, the correlation between RH_dry profile (pink line in Fig.6c) and its corresponding σ_{sca} was r^2=0.62, where r is the correlation coefficient (Fig.8a).

- **Section 4.2:**

11. Again, which flights/spirals/dates were identified as polluted? How did you define polluted?

Reply: Polluted flights/spirals on different days include RF5 (on May 19, spirals at LC), RF6 (on May 21, spirals at QZ, XT), RF7 (on May 28, spirals at JL, XT), RF8 (on May 28, spirals at XT), and 21 vertical profiles in total were identified as pollution in the lower layer of PBL. We define polluted PBL by the mean value of σ_{sca} greater than 100 Mm^{-1} in the PBL layer and high levels of gas pollutants like CO and NOx were observed. Weather phenomenon (Table 1) at flight time was also one of the considered factor. Three typical types of polluted PBL are classified according to the shapes of σ_{sca} vertical profiles. Fig.6b shows the vertical profiles of σ_{sca} of pollution in the lower layer of the PBL. The profiles of this type show that the gradient of σ_{sca} are generally small from surface to a certain layer (H_{PBL}), then the value of σ_{sca} sharply decreased.

12. It seems like you fit Eq 7 to the data. Please state this explicitly. What method did you use to derive this fit?

Reply: As mentioned in previous paragraphs, the structure of PBL is a crucial factor, which determines the vertical distribution of aerosol property in the lower troposphere. The types of PBL structure are classified by the shapes of σ_{sca} profiles. To better show the similarity of these profile shapes, the PBL heights of different profiles have been adjusted to the same level (Fig.6b).

According to previous study of aerosol vertical distribution, e.g. Liu et al. (2009), we use linear fit to represent the σ_{sca} distribution in the PBL and use curve fitting (exponential function) to represent σ_{sca} profiles in the free troposphere.

We have added the following description in Section 4.2 in the revised manuscript.

$$\sigma_{sca,\,H}=\begin{cases}\sigma_{sca,\,PBL}\cdot\exp(-(H-H_{PBL})/H_p), & (\text{if } H > H_{PBL})\\ \sigma_{sca,\,0}+k\cdot H, & (\text{if } H \le H_{PBL})\end{cases}, \quad (9)$$

where H_{PBL} is the normalized altitude of PBL height, H_p is the aerosol scale height in the free troposphere, k is the changing rate of σ_{sca} in the PBL. In these cases, $\sigma_{sca,0}$=171 Mm^{-1}, H_p =216 m, k= 0.03 Mm^{-1} m^{-1} and r^2=0.9394. Fig. 6d shows the ambient RH profiles under dry and humid conditions. The shapes of dry and humid RH profiles were similar in the PBL, but at the top of the PBL, the RH_dry profiles dramatically decreased while the RH_humid profiles slightly changed. Linear fits were made to determine the correlation between RH and σ_{sca}. Under dry condition, there was a pronounced correlation (r^2=0.95) between RH_dry and σ_{sca} profiles. But under humid condition, the correlation coefficient was 0.12, which suggest a poor correlation between RH_humid and σ_{sca} profiles.

13. Does the scatter plot in Fig 9b include both dry and humid profiles? Please state explicitly.

Reply: Yes, the scatter plot in Fig.9b (now Fig.8b in the revised manuscript) include both dry and humid profiles, but only in the lower layer of PBL ($H < H_{PBL}$). We have made a change to Fig. 8 and added some description in Section 4.2 in the revised manuscript. Now, the Fig.8b showed a linear regression analysis and the correlation coefficient between RH_dry and σ_{sca} profiles (corresponding to the blue line of RH_dry in Fig. 6d).

14. You seem to contradict yourself, by first saying that both dry and humid profiles have good correlation between RH and σsca, then above the PBL only dry profiles are correlated. Please clarify.

Reply: Thanks for your comment. As we mentioned above, under dry condition, there was a pronounced correlation (r^2=0.95) between RH_dry and σ_{sca} profiles. While under humid condition, the correlation coefficient was 0.12, which suggest a poor correlation between RH_humid and σ_{sca} profiles.

However, if the constraint is PBL height，the correlation between RH and σ_{sca} was r^2=0.78 (below PBL height, $H \le H_{PBL}$) and r^2=0.07 (above PBL height, $H > H_{PBL}$), both of them including dry and humid profiles. To better explain it, we have added the following description in Section 4.2 in the revised manuscript.

“Linear fits were made to determine the correlation between RH and σ_{sca}. Under dry condition, there was a pronounced correlation (r^2=0.95) between RH_dry and σ_{sca} profiles. But under humid condition, the correlation coefficient was 0.12, which suggest a poor correlation between RH_humid and σ_{sca} profiles.”

- **Section 4.3:**

15. Did the upper-layer and multi-layer profiles only occurs on these two days?

Reply: Yes, we found such types of PBL structure only on these two days during the experimental period and each type includes 2 profiles.

16. At which location were these profiles measured?

Reply: The profiles were measured at LC (RF9 on June 2 with 2 spirals) and JL (RF10 on June 6 with 2 spirals), respectively. We have included the location information in caption of Fig. 7.

17. Figs 9c and 9d refer to these profiles, not 9a and 9b. Do you only include data from those two dates/profiles in Fig 9c and 9d. Please clarify.

Reply: Thanks for your comment, we correct the mistake in the revised manuscript. The Fig.9c and 9d (now Fig. 8c and 8d) include data measured at LC (RF9, 2 profiles) and JL (RF10, 2 profiles). We have clarified the two dates in the caption of Fig. 8. The scatter, the horizontal and vertical error bars represent mean values and the standard deviations of RH and σ_{sca} at every 100 m level.

18. Section 4 in general only considers aerosol scattering. What about absorption? Angstrom exponent? How are these aerosol properties affected by different transport patterns?

Reply: The σ_{abs} and Angstrom exponent profiles are shown in the following figure. According to the polluted conditions mentioned above, four types of profiles are classified by their different shapes. Liner regression shows the correlation between σ_{abs} and its corresponding ambient RH are r^2=0.24, 0.62, 0.57, 0.31, respectively, which was not exactly the same as σ_{sca} we discussed in the paper. Furthermore, the σ_{abs} scatters in second type under different RH condition, r^2=0.66 (between σ_{abs} and RH, under dry condition) and r^2=0.01 (under humid condition). Compared with σ_{sca}, the σ_{abs} has less correlation with ambient RH. Similar method was used to discuss the Angstrom exponent profiles in Fig.2, but the correlation is substantially poorer from the result.

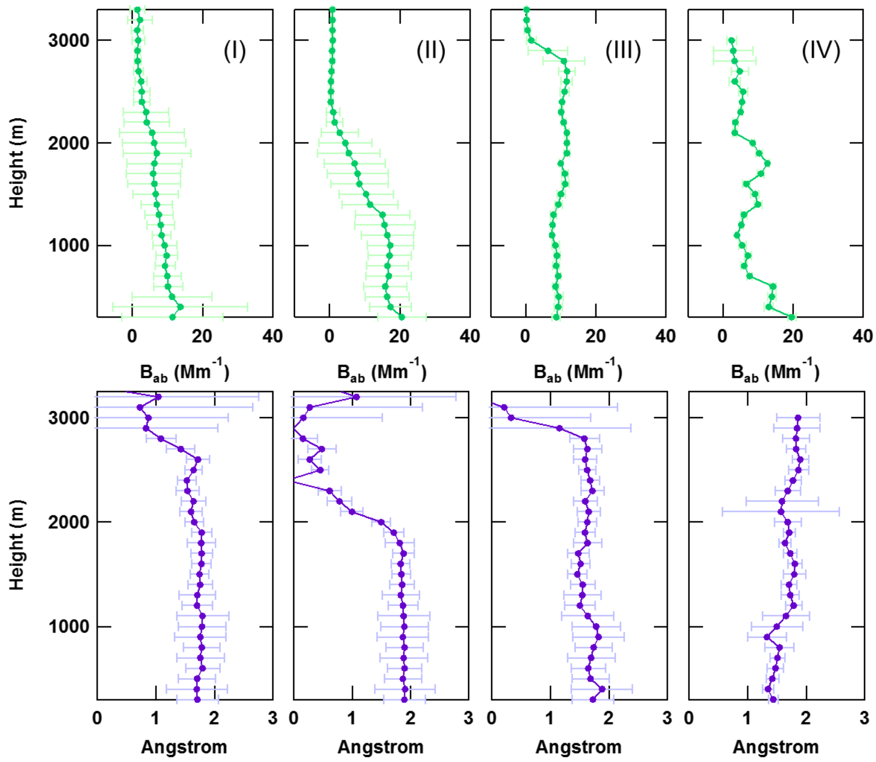

Fig.2 Different types of aircraft-measured vertical profiles of σ_{abs} (green line) and Angstrom exponent (purple line). Horizontal error bars represent the standard deviations at every 100m level.

Cluster analysis of 72 hours HYSPLIT back-trajectories were carried out to discuss the influence of aerosol optical properties by different transport pattern. Taking absorption coefficient as an example, the long-range transport from north (89%) was the dominate type and the local air mass contribute a fraction of σ_{abs} (8%), as shown in Fig.3a (corresponding to type I in Fig.2). In contrast, if σ_{abs} profile was approximate to the profiles in Fig.2 (II), the enrichment of light-absorbing aerosols in the upper layer of the PBL show that the moist and polluted air masses from interior and coastal areas are dominated (83%) during the field campaign. However, the long-range transport of aerosols was not significant.

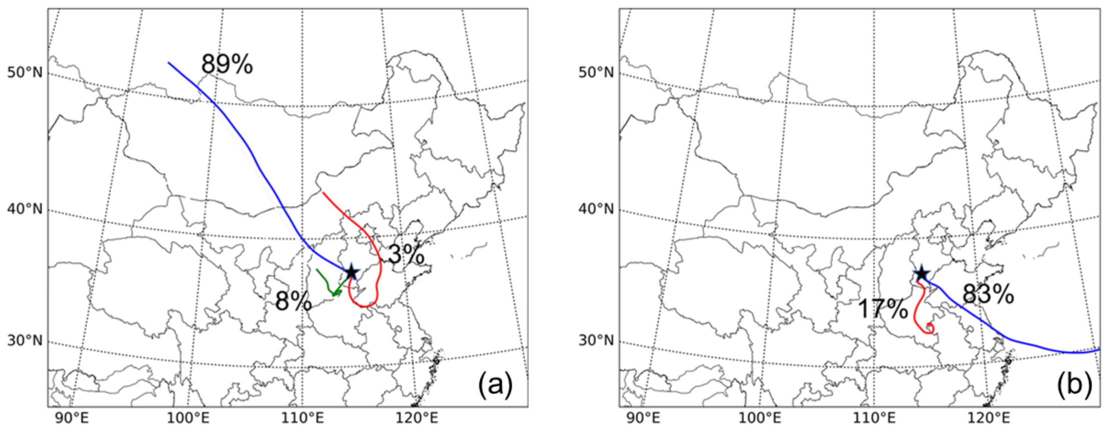

Fig.3 Cluster analysis of 72 hours HYSPLIT back trajectories for the σ_{abs} profiles in Fig.2 (a:

corresponding to I type and b: corresponding to II type)

- **Technical Corrections:**

Reply: Thanks for your careful review. These have been corrected in the revised manuscript.

References:

Fan, J., Rosenfeld, D., Yang, Y., Zhao, C., Leung, L. R., and Li, Z.: Substantial contribution of anthropogenic air pollution to catastrophic floods in Southwest China, Geophysical Research Letters, 42, 6066-6075, 2015.

Li, X., Zhang, Q., Zhang, Y., Zheng, B., Wang, K., Chen, Y., Wallington, T. J., Han, W., Shen, W., and Zhang, X.: Source contributions of urban PM 2.5 in the Beijing–Tianjin–Hebei region: Changes between 2006 and 2013 and relative impacts of emissions and meteorology, Atmospheric Environment, 123, 229-239, 2015.

Liu, P., Zhao, C., Zhang, Q., Deng, Z., Huang, M., Xincheng, M. A., and Tie, X.: Aircraft study of aerosol vertical distributions over Beijing and their optical properties, Tellus Series B-chemical & Physical Meteorology, 61, 756–767, 2009.

Sun, X., Yin, Y., Sun, Y., Sun, Y., Liu, W., and Han, Y.: Seasonal and vertical variations in aerosol distribution over Shijiazhuang, China, Atmospheric Environment, 81, 245-252, 2013.